NEUTRON PRODUCTION MEASUREMENTS RELEVANT TO SHIELDING FOR SPACE-RELATED ACTIVITIES

Lawrence Heilbronn
Lawrence Berkeley National Laboratory

Yoshiyuki Iwata, Takeshi Murakami
National Institute of Radiological Studies

Hiroshi Iwase, Takashi Nakamura, Hisaki Sato
Tohoku University

Reginald Ronningen
National Superconducting Cyclotron Laboratory

DISCLAIMER

Abstract

Neutron production cross sections have been measured from 290 MeV/nucleon C and 600 MeV/nucleon Ne interacting in a slab of simulated Martian regolith/polyethylene composite, and from 400 MeV/nucleon Ne interacting in a section of wall materials from the International Space Station. Neutron spectra were measured at 7 angles between 5º and 80º, and for neutron energies 5 MeV and greater. Spectra at forward angles are dominated by the breakup of the projectile, whereas spectra at back angles show the typical exponential falloff with energy that is indicative of decay from the overlap region and the target remnant. The measured total neutron production cross sections indicate that the regolith/polyethylene composite may be a more effective shielding material than the ISS wall materials, in terms of the number of neutrons produced.

Introduction

One of the primary limiting factors to long-term human space operations is the health risk to the astronaut from the exposures to the space ionizing radiation environment. The establishment of a permanent human presence on the International Space Station and the exploration and settlement of the moon and Mars are examples of such mission scenarios. The ultimate limitation on long-term operations is maintaining the radiation induced cancer risks to acceptable levels. The most effective means to reduce radiation exposures is the use of intervening materials to reduce the radiation intensity within an enclosed structure.

The space ionizing radiation environment is very complex, consisting of a low-level background of galactic cosmic radiation (GCR), transient solar particle events (SPE), and, while in Earth orbit, the trapped radiation belts. As these radiations traverse shielding materials they interact with the materials through specific atomic and nuclear processes, including breaking up the ions into smaller fragments and producing secondary radiation that can penetrate more deeply into the material. The composition and intensity of these transmitted radiations (secondaries and fragments) depend on the elemental constituents of the specific materials. The radiation-induced injury in biological tissue depends on the composition and intensity of the transmitted particles. An extremely important secondary particle component in this respect is the neutron, which has no charge and is not reduced in atomic interactions but is extremely damaging to biological tissue. Current theoretical models have shown the secondary neutrons to be a major contributor to exposures within lunar habitats and on the Martian surface, and recent studies have shown that neutrons could comprise 30 to 60 percent of the dose equivalent on the ISS. A recent review of the neutrons in the Earth's atmosphere has raised serious questions about the adequacy on our understanding of the production and propagation of neutrons by GCR in atmospheric components. Any advances on the specification of shielding for habitats on the moon or Mars require measurements on the transmitted neutron component within lunar and Martian shielding materials and improvements on databases and computational procedures.

The National Aeronautics and Space Administration of the United States is currently supporting a ground-based research program to study the effects of Galactic Cosmic Ray (GCR) transport through spacecraft materials and human tissue. The goal of the program is to provide a reliable database of relevant nuclear cross sections and thick target yields for the development of and verification of transport model calculations used for low-Earth orbit and deep space shielding design. Ions with $Z \geq 2$ make up approximately 12% of the GCR flux; however, previous calculations indicate that neutron production from heavy-ion interactions in shielding materials may contribute at least 30% of the total neutron flux. Our group has measured several neutron production cross sections that are relevant to heavy-ion GCR transport through shielding materials. In this paper we present cross sections from

two specialized NASA targets: (1) A slab of simulated Martian regolith mixed with polyethylene, referred to herein as "Marsbar", and (2) a section of wall from the International Space Station (ISS).

Experimental Details

The experiments were carried out at the Heavy Ion Medical Accelerator in Chiba (HIMAC) facility at the National Institute of Radiological Sciences, Chiba, Japan. HIMAC delivered beams of 290 MeV/nucleon C, 400 MeV/nucleon Ne, and 600 MeV/nucleon Ne to targets placed along the PH2 beam course. The 290 AMeV C and 600 AMeV Ne beams were incident upon the Marsbar, and the 400 AMeV Ne was incident upon the ISS wall section. Table 1 summarizes the beam-target information from each run, including the beam energy at midpoint in the target. The midpoint energy is used as the relevant beam energy from this point on.

Table 1. Beam and target combinations

Beam	Energy	Target	Thickness
C	265 AMeV	Marsbar	5 g/cm^2
Ne	380 AMeV	ISS wall	3 g/cm^2
Ne	570 AMeV	Marsbar	5 g/cm^2

The Marsbar is comprised of 85% simulated Martian regolith and 15% polyethylene. Table 2 shows the atomic parameters of a represenative sampling of Martian regolith. The ISS wall is comprised of 1.89 g/cm^2 of aluminum, 0.218 g/cm^2 of Nomex® honeycomb wall, 0.08 g/cm^2 of Nomex® cloth, 0.06 g/cm^2 Durette® batting, and 0.72 g/cm^2 silicone rubber.

Table 2. Martian regolith composition

Element	Atomic density (atoms/g)
O	1.67×10^{22}
Mg	1.62×10^{21}
Si	5.83×10^{21}
Ca	7.81×10^{20}
Fe	1.80×10^{21}

Beam was delivered every 3.3 seconds in pulses that lasted between 0.6 and 1second. Beam intensity was between 10^4 to 10^5 ions per pulse. In general, live time was on the order of 60 to 90 percent.

Immediately after exiting the beam-line vacuum system, the beam passed through a 0.5-mm thick plastic scintillator, referred to as the trigger detector. The trigger detector was used to count the number of incident ions, as well as reject any pile-up events. The targets were placed approximately 5 cm downstream from the beam scintillator. After passing through the target, the beam traveled about 20 m through air before stopping in a beam dump.

The neutron detectors used were cylinders (12.7 cm in diameter and 12.7 cm in depth) of liquid scintillator (NE 213). Seven detectors were placed at 5°, 10°, 20°, 30°, 40°, 60°, and 80° in the lab. Flight paths from target center to detector center varied between 306 and 506 cm. A 5-mm thick, solid-plastic scintillator was placed directly in front of each neutron detector. Those scintillators were used to reject any events due to charged particles incident upon the accompanying neutron detector.

Gamma-ray events were distinguished from neutron events by using the pulse shape difference between those two type of events

Neutron energies were measured by time of flight. The time difference between corresponding signals in the trigger detector and neutron detector was recorded for each event. For neutron detectors placed 506 cm from the target, the overall energy resolution was 8%, 11%, and 14% for 200, 400 and 600 MeV neutrons, respectively. For the 306-cm flight path, the corresponding energy resolutions were 13%, 18% and 23%, respectively. Background neutrons were measured using the shadow-bar technique. Additional information regarding experimental details may be found in reference 1.

Results

Figures 1-3 show the double-differential neutron production cross sections from the three systems, at the indicated angles. In order to clearly present the data, the spectra have been multiplied by successive factor of 0.1 as angle increases. At forward angles, the spectra are dominated by neutrons produced in the breakup of the projectile. Because of the kinematical boost from Fermi momentum, neutron energies greater than two times the incoming beam energy per nucleon are detected. The lower threshold on neutron energy is 5 MeV for all the spectra. The error bars show the statistical uncertainties, only. The systematic uncertainties are being determined at the time of this writing, and are estimated to be between 20 to 50 percent. As angle increases from 5º to 30º, the contribution from projectile breakup becomes less significant. At large angles, the spectra exhibit an exponential falloff with energy. The exponential behavior indicates that the spectra there are dominated by the decay of the target remnant and the overlap region between the target and projectile.

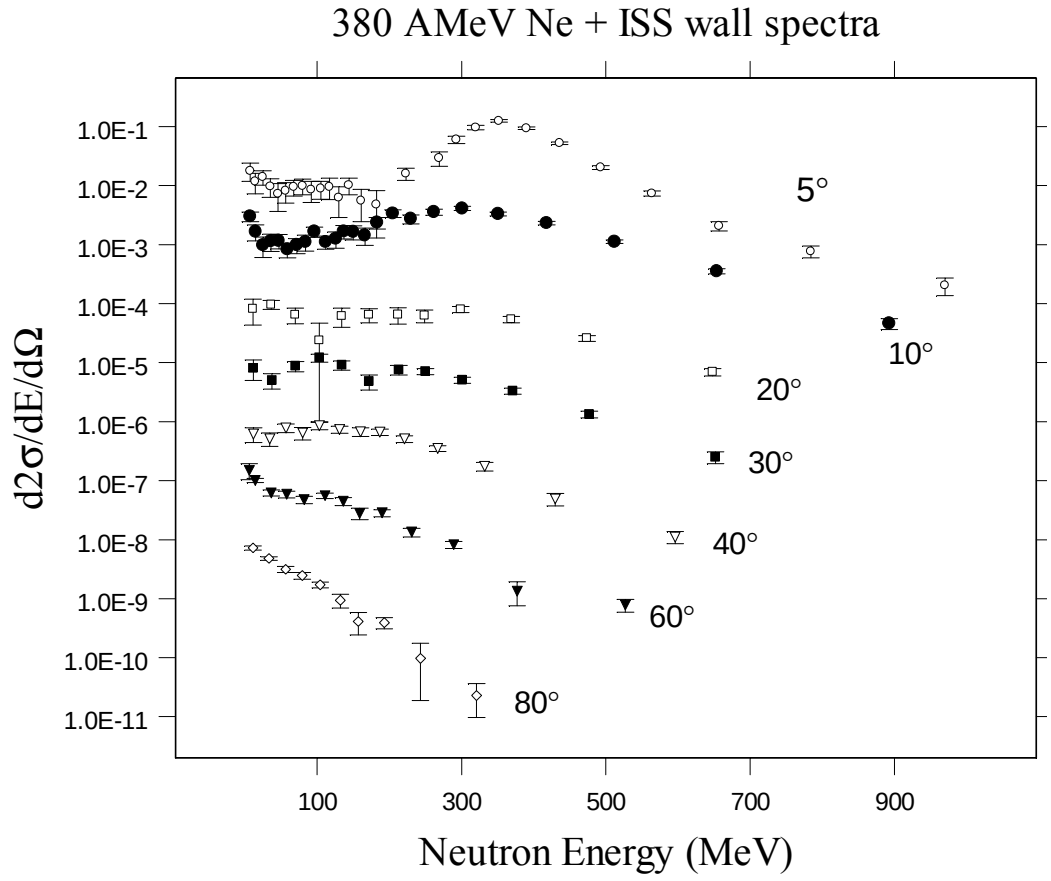

Figure 1. Double-differential spectra from 380 AMeV Ne + ISS wall (unpublished).

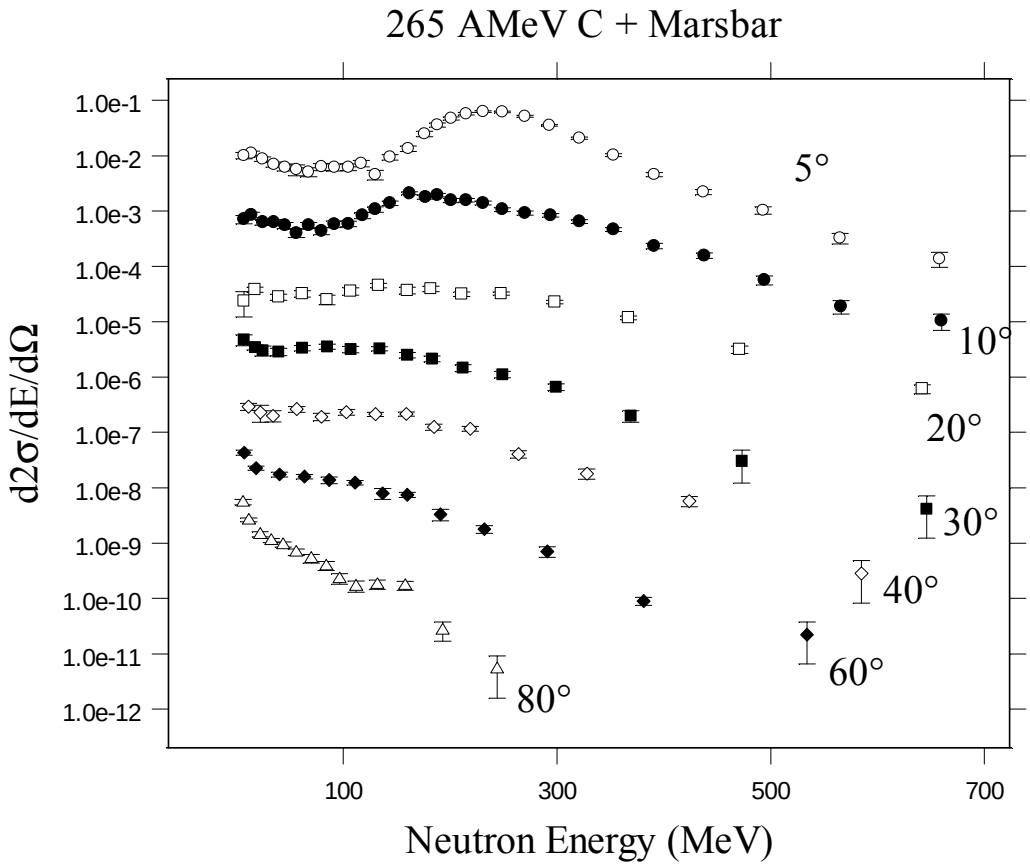

Figure 2. Double differential spectra from 265 MeV/nucleon C + Marsbar system (unpublished).

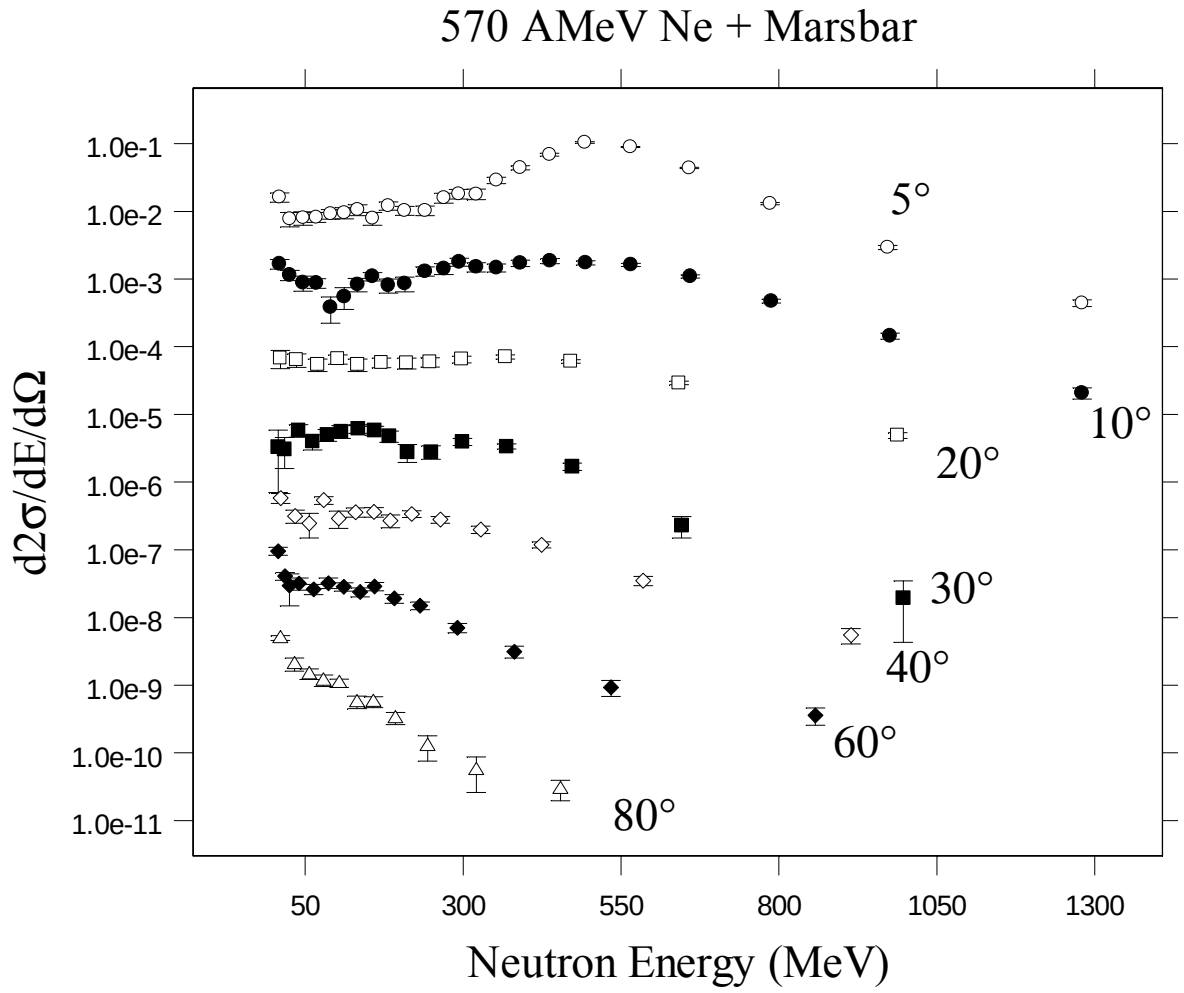

Figure 3. Double-differential neutron spectrum from 600 MeV/nucleon Ne +Marsbar (unpublished).

The double-differential spectra, such as the one in Figs. 1-3, can be integrated over energy to yield angular spectra. Figure 4 shows the angular distribution between 5º and 80º from all three systems, for neutron energies 5 MeV and greater. The error bars indicate statistical uncertainties, only. The distribution shown in Fig. 2 is typical of such neutron angular spectra from heavy-ion interactions.[1,2] The spectra are forward-peaked, and can be fitted with the sum of two exponentials. The point where the contributions from both exponentials are equal is dependent upon the incoming beam momentum per nucleon.[2]

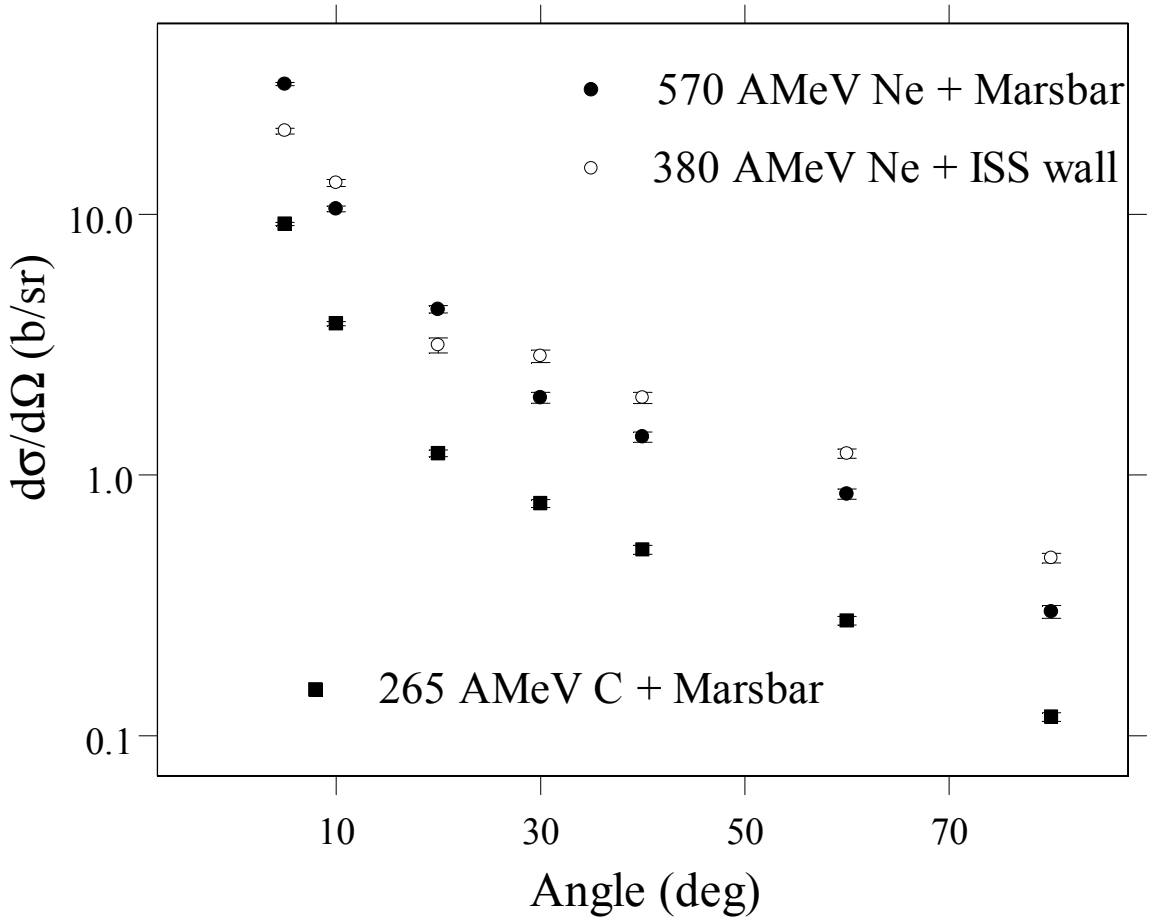

Figure 4. Neutron angular distribution from all three systems (unpublished).

Figure 5 shows the neutron energy distribution from all three systems. To generate this spectrum, the 5º spectrum was assumed to cover the range between 0º and 7.5º, the 10º spectrum ranges between 7.5º and 15º, the 20º spectrum ranges between 15º and 25º, the 30º spectrum ranges between 25º and 35º, the 40º spectrum ranges between 35º and 50º, the 60º spectrum ranges between 50º and 70º, and the 80º spectrum ranges between 70º and 90º. This spectrum can then be integrated over energy to yield the total neutron production cross section.

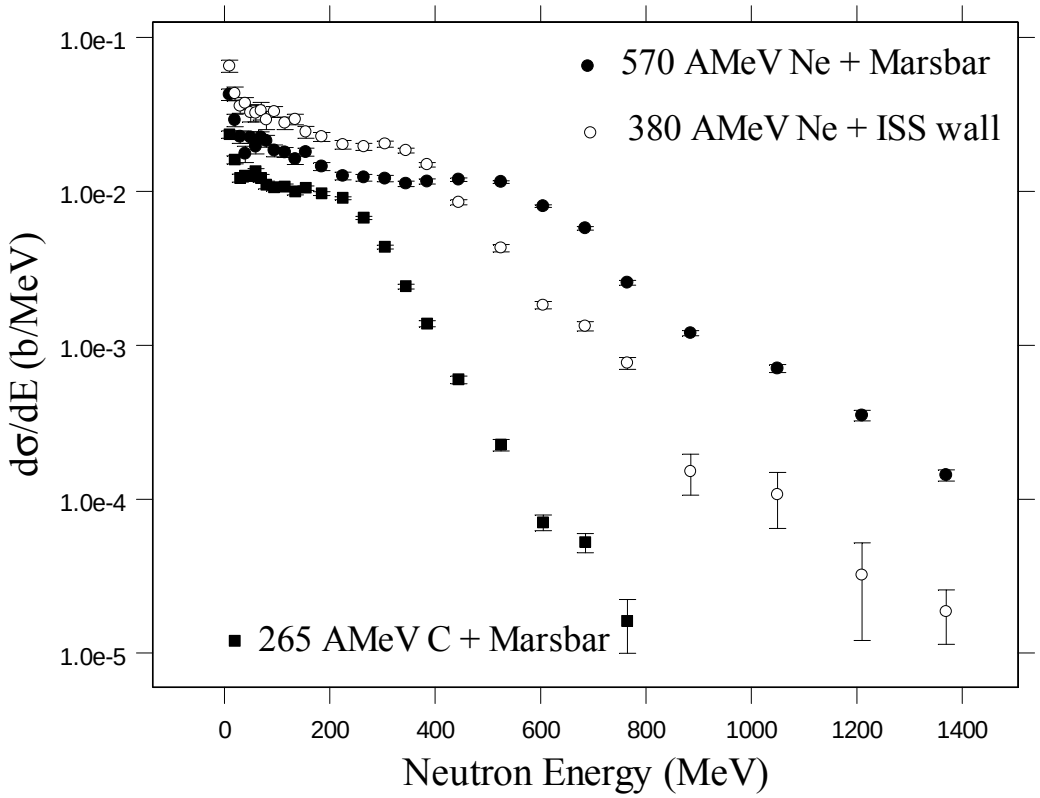

Figure 5. Energy spectra from all three indicated systems (unpublished).

The total neutron production cross section is 3.4 barns for 290 AMeV C + Marsbar, 9.9 barns for 600 AMeV Ne + Marsbar, and 10.5 barns for 400 AMeV Ne + ISS wall. Comparison of these total neutron cross sections with those reported in Ref. 1 are shown in Table III, and indicate that the Marsbar and ISS wall materials have an effective elemental mass between C and Cu, at least in terms of neutron production. Assuming a linear relationship between total neutron production cross section and elemental mass, the Marsbar has an effective mass number of about 30, whereas the ISS wall has an effective mass number of 40. Both the Marsbar and the ISS wall used in the experiments are relatively thick, and as such there may be a need to correct for target thickness in order to extract "true" cross sections. In any case, this analysis indicates that the Marsbar may be more effective in limiting neutron production than the ISS wall. These preliminary results indicate that building materials with light-mass elemental components may be the most effective in reducing the number of neutrons produced from interactions with the heavy ions present in space radiation.

Table III. Total neutron production cross sections (0º-90º), in barns (unpublished).

	Targets				
Beam	Carbon	Marsbar	ISS Wall	Cu	Pb
290 AMeV C	1.9 b	3.4 b		6.1 b	22.1 b
400 AMeV Ne	4.4 b		10.5 b	15.8 b	52.8 b
600 AMeV Ne	3.7 b	9.9 b		18.7 b	57.2 b

ACKNOWLEDGMENTS

The authors wish to acknowledge the HIMAC staff for their support and efficient operation of the accelerator. This work was supported by the U.S. National Science Foundation under Grant No. 95-28844, NASA Contract No. H-29456D and Grant No. L14230C through the U.S. DOE under Contract No. AC03076SF00098.

REFERENCES

1. Y. Iwata, T. Murakami, H. Sato, H. Iwase, T. Nakamura, T. Kurosawa, L. Heilbronn, R. M. Ronningen, K. Ieki, Y. Tozawa, and K. Niita, "Double-differential cross sections for the neutron production from heavy-ion reactions at energies E/A = 290-600 MeV", *Phys. Rev. C,* Volume 64, 054609, (2001).

2. L. Heilbronn, R. Madey, M. Elaasar, M. Htun, K. Frankel, W. G. Gong, B. D. Anderson, A. R. Baldwin, J. Jiang, D. Keane, M. A. McMahan, W. H. Rathbun, A. Scott, Y. Shao, J. W. Watson, G. D. Westfall, S. Yennello, and W. –M. Zhang, "Neutron yields from 435 MeV/nucleon Nb stopping in Nb and 272 MeV/nucleon Nb stopping in Nb and Al", *Phys. Rev. C,* Volume 58, no. 6, pages 3451 - 3461 (1998).